

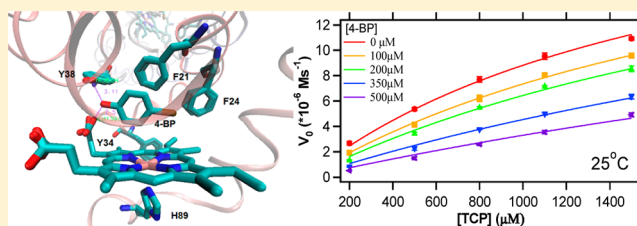
Kinetic Study of the Inhibition Mechanism of Dehaloperoxidase-Hemoglobin A by 4-Bromophenol

Jing Zhao and Stefan Franzen*

Department of Chemistry, North Carolina State University, Raleigh, North Carolina 27695, United States

S Supporting Information

ABSTRACT: The mechanism of dehaloperoxidase-hemoglobin (DHP) inhibition by 4-bromophenol (4-BP) was investigated using Michaelis-Menten and transient-state kinetic analyses. Transient-state kinetics using the stopped-flow technique to mix DHP and H_2O_2 in the presence of inhibitor concentrations less than 10-fold greater than the enzyme concentration show that 4-BP does not fully impede H_2O_2 entering the distal pocket to activate DHP. It is not clear whether an oxoferryl intermediate is formed under these conditions and there may be alternative pathways for H_2O_2 reaction in the 4-BP bound form of DHP. Two new species have been identified during the reaction of 4-BP bound form of DHP in the transient-state kinetic experiment by using Singular Value Decomposition (SVD) and global-fitting analysis. Rather than forming Compound ES in the unbound form, an inhibitor bound intermediate that possesses blue-shifted Soret band and a double peaked Q-band is observed. This intermediate is subsequently converted to the end-point species that is distinguished from Compound RH formed in the uninhibited enzyme. Bench-top mixing kinetics of DHP were conducted in order to determine the inhibitor binding constant and to understand the enzyme inhibition mechanism from a thermodynamic perspective. It was found that the inhibition constant, K_i , decreased from 2.56 mM to 0.15 mM over the temperature range from 283 to 298 K, which permits determination of the enthalpy and entropy for inhibitor binding as -135.5 ± 20.9 kJ/mol and 526.1 ± 71.9 J/(mol·K), respectively, leading to the conclusion that inhibitor binding is entropically driven.

**INTRODUCTION**

Dehaloperoxidase-hemoglobin A (DHP A) isolated from *Amphitrite ornata* is the first known hemoglobin with a biologically relevant peroxidase function for 2,4,6-tribromophenol (2,4,6-TBP) as a substrate.¹ There are two globin genes in *A. ornata*, and the second gene product DHP B is a 3-fold better peroxidase than DHP A.² Both DHP A and DHP B (collectively called DHP) appear to have multiple functions, which has made them the focus of intensive investigation. While it is not possible yet to determine how the function of DHP relates to the evolution of function in the peroxidase superfamily,³ inhibition by 4-bromophenol (4-BP) provides one unique feature of DHP that provides a crucial clue as to the functional origins of the enzyme.⁴ Due to its ability to oxidize halophenols and other halogenated substrates in the presence of H_2O_2 in nature, DHP also has a potential application in bioremediation strategies to degrade halogenated organic pollutants produced by anthropogenic activity.⁵ However, it is imperative to understand the role of inhibition in order to optimize the activity of DHP both to understand its physiological role in *A. ornata* and for bioremediation applications.

DHP activity has been shown to depend upon both pH and chemical modifications of the substrate.^{6,7} Unlike secretory peroxidases, which have optimum function at pH 5, DHP has shown maximal activity at pH 7.5, which is commensurate with

the pH of cytosol. This pH dependence is consistent with a role for DHP as a peroxidase in the coelom of *A. ornata* and makes DHP similar to other class I peroxidases such as ascorbate peroxidase or cytochrome c peroxidase.⁸ However, DHP has a globin protein fold and it is not known whether the peroxidase function arose from convergent evolution of the globin⁹ or whether DHP has some of the properties of an ancient multifunctional hemoglobin that may be postulated to have existed, based on phylogenetic analysis.¹⁰

Previous studies have also shown that trihalophenols (2,4,6-TXP), such as 2,4,6-TBP, 2,4,6-TCP, and 2,4,6-TFP are significantly better substrates than the monohalophenols, 4-BP, 4-CP, and 4-FP.¹¹ In fact, 4-BP has very low turnover and can act as a potent inhibitor for other substrates.¹² This point is relevant to the biological function of DHP since the native substrate 2,4,6-TBP and apparent inhibitor 4-BP are present in benthic ecosystems in a ratio of approximately 1:2.¹³ Recent study reveals the diameter of the halogen atom in the para position plays a crucial role in the binding of 4-halophenols in the distal pocket.¹⁴ 4-Halophenols with smaller halogen atoms, chlorine or fluorine, in the para position do not bind as well, and thus 4-CP and 4-FP are not as effective as inhibitors. For

Received: November 26, 2012

Revised: June 8, 2013

Published: June 10, 2013

example, although 4-BP is an excellent inhibitor and poor substrate, 4-CP shows considerable activity as a substrate.^{12,14} The biological significance can be approached by first understanding the thermodynamics and kinetics of inhibitor binding, which motivates the present study.

The oxidation of 2,4,6-TCP by DHP serves as an excellent model for DHP A activity.^{2,11,15–18} The choice of 2,4,6-TCP, rather than the native substrate 2,4,6-TBP was motivated by the poor solubility of 2,4,6-TBP, which limits the ability to determine the initial rate as a function of substrate concentration, and therefore renders Michaelis–Menten kinetic analysis meaningless. The substrate, 2,4,6-TCP, and inhibitor, 4-BP, appear to have distinct binding sites, exterior and interior, respectively.^{7,12} Both Raman spectroscopic measurements and X-ray crystal structures show that the 2,4,6-TCP substrate binding site is not located in the internal binding site above the heme, but rather 4-XPs bind at that internal site.¹² Based on resonance Raman data it has been hypothesized that substrate binding appears to occur at an external binding site at the heme edge, as is typical of substrate binding in peroxidases.¹⁹ Further support for these models has been obtained from ¹H–¹⁵N HSQC experiments, which show different binding interactions between 2,4,6-TCP and 4-BP based on the pattern of chemical shifts in the protein backbone for each molecule.²⁰ Binding of 4-BP generated the largest deviation in backbone chemical shift in the distal pocket, while binding of 2,4,6-TCP produced the greatest deviation close to the DHP dimer interface around the amino acid residue Trp¹²⁰ and the flexible distal histidine, His⁵⁵.

Despite the strong experimental evidence for an external substrate binding site, recent X-ray structures of substrate infused into preformed crystals revealed that there is also an internal binding site for 2,4,6-TBP above the heme α -edge.²¹ This site is distinct from the inhibitor binding site. Thus, it is structurally consistent with the two-site competitive inhibition model, although the implications are quite different than for the external substrate binding site.¹¹ We know further based on studies of oxy DHP that the binding of substrate also has the effect of triggering a functional switch from oxygen transport (hemoglobin) to oxidative (peroxidase) function.²² The new information obtained from these studies requires a more detailed investigation of the thermodynamics of inhibitor binding in order to understand the interplay between the various modes of binding.

The previously proposed inhibition mechanism that involves 4-BP binding in the distal pocket has consequences for peroxidase function.²² When 4-BP is bound in the internal binding site above the heme the distal histidine, His⁵⁵, is displaced to a solvent-exposed conformation, in which distal His⁵⁵ is too far away from the heme center to function as an acid–base catalyst that can facilitate O–O heterolysis of H₂O₂. Heterolytic bond cleavage is essential for the formation of Compound I or Compound ES, which is the first intermediate formed in typical peroxidases such as horseradish peroxidase (HRP)^{23,24} or cytochrome c peroxidase (CcP).^{25,26} DHP has been shown to form a Compound ES intermediate when substrate is not present,²⁷ which has been shown to involve one or more tyrosine radicals.^{2,28} Based on the kinetic data it appears that the tyrosine radical observed transiently in DHP is not an electron transfer intermediate, but rather may play a protective role. The end point for the radical chemistry in the absence of substrate is an inactive (or at least severely impaired) cross-linked heme species called compound RH.²⁹ The relationship between the internal radical pathways and

compound RH formation with normal function has not been established.

To probe the 4-BP inhibition mechanism of DHP, we have conducted a transient-state kinetic study of the reaction between ferric enzyme and H₂O₂ for a range of 4-BP concentrations using a stopped-flow UV–visible spectrophotometer. Two parallel reactions with 4-BP bound and unbound DHP were observed using singular value decomposition (SVD) and global fitting analysis of stopped-flow data. Thus, a novel inhibition mechanism was proposed based on the presence of this equilibrium. A comprehensive benchtop kinetic study of DHP catalytic process in the presence of the inhibitor 4-BP was conducted at a variety of temperatures following methods developed previously. The benchtop kinetic data have been fit to a simplified inhibition kinetic model in order to determine the inhibition constant K_i and its temperature dependence, which provides the thermodynamics of the binding of 4-BP to DHP. The kinetic measurements and analysis presented here provide further support for the novel inhibition mechanism of DHP.

■ MATERIAL AND METHODS

Materials. All the reagents and biochemicals were purchased from Aldrich and ACROS and used without further purification. 2,4,6-Trichlorophenol (TCP) and 4-Bromophenol (4-BP) were each dissolved in 100 mM, pH = 7 potassium phosphate (KP_i) buffer to prepare the substrate and inhibitor solution. Prepared solutions were stored at 4 °C and protected against light. The concentration of each solution was measured prior to each kinetic experiment by monitoring its absorbance: TCP, $\epsilon_{312\text{ nm}} = 3752\text{ M}^{-1}\text{ cm}^{-1}$; 4-BP, $\epsilon_{280\text{ nm}} = 1370\text{ M}^{-1}\text{ cm}^{-1}$ in Agilent 8453 diode array UV–visible spectrophotometer at 25 °C. Hydrogen peroxide solution was freshly made before each kinetic experiment. A 30% reagent grade hydrogen peroxide (H₂O₂) solution was added to 100 mM, pH = 7 KP_i buffer to make a 7.2 mM stock solution. The hydrogen peroxide solution was kept on ice and protected against light during the experiment. Wild-type His6X DHP A was expressed in *E. coli* and purified as previously described.¹⁸ Ferric DHP was oxidized by excess K₃[Fe(CN)₆] and then filtering through Sephadex G-25 column to eliminate excess K₃[Fe(CN)₆] and further purified on CM-52 prior to each kinetic experiment. The concentration of ferric DHP was determined by using the Soret band molar absorption coefficient, $\epsilon_{406\text{ nm}} = 116,400\text{ M}^{-1}\text{ cm}^{-1}$.

Transient-State Kinetic Assays. Experiments were performed on a Bio-Logic SFM-400 triple-mixing stopped-flow instrument equipped with a diode array UV–visible spectrophotometer and were carried out at room temperature in 100 mM KP_i buffer, pH 7. Data were collected over three time-domain regimes (2.5, 25, and 250 ms; 300 scans each) using the Bio Kinet32 software package (Bio-Logic). Data were collected (900 scans total) over a three-time domain regime (2.5, 25, and 250 ms; 300 scans each, 83.25 s total) using Bio Kinet32 (Bio-Logic). Single-mixing experiments were performed, in which ferric DHP was preincubated with 4-BP prior to the mixing with H₂O₂. The final concentrations after mixing were [DHP] = 10 μM , [H₂O₂] = 100 μM , and [4-BP] ranging from 0, 10, 20, 100 μM .

Benchtop Mixing Kinetic Assays. The kinetic assays were conducted in 100 mM, pH = 7 KP_i buffer using an Agilent 8453 UV–visible spectrophotometer equipped with Peltier temperature controller. The catalytic reactions were carried out in a 0.4

cm path length cuvette obtained from Starna Cells, Inc., with a total volume of 1200 μL . The ferric DHP concentration $[E]_0$ in each sample was 2.4 μM . Substrate, 2,4,6-TCP, concentrations ranged from 200 to 1500 μM , and inhibitor, 4-BP, concentrations ranged from 0 to 500 μM . The substrate and inhibitor were first mixed with ferric DHP and KP_i buffer and then allowed to incubate for 3 min in the cuvette placed in the thermal cell to reach thermal equilibrium. Subsequently, 1200 μM of H_2O_2 solution was added into the cuvette to initiate the reaction. The kinetic data were measured by monitoring the absorbance at wavelength 273 nm, which corresponds to the absorbance peak of the 2,6-dichloroquinone (DCQ) product, with a molar absorption coefficient $\epsilon_{273\text{ nm}} = 13,200\text{ M}^{-1}\text{ cm}^{-1}$.

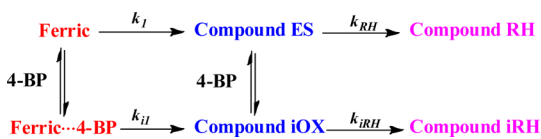
Data Analysis. Spectra measured using a stopped-flow kinetic assay were analyzed using the SVD method, which provides a decomposition of the original absorption data matrix $A(\lambda, t)$ in terms of basis spectra as the product of three matrices USV^T .^{30,31} As described in detail in the Supporting Information, the first three vectors in the V^T matrix (Figure S2) correspond to the time-courses of the reaction orthonormal basis spectra given in the U matrix (Figure S1) for the reaction in the absence of 4-BP. The time courses were globally fit to a biexponential function according to the proposed two-step three-species first order reaction mechanism shown in Scheme 1, from which the rate constants k_I , k_{RH} and the 3×3 C coefficient matrix were determined.

Scheme 1. Kinetic Model for the Global-Fitting Analysis of the Stopped-Flow Data in the Absence of 4-BP



In the presence of 4-BP, the V^T matrix (Figure S4) was evaluated as two parallel two step reactions since there are two populations of DHP A proteins. Population 1 has a bound 4-BP inhibitor and population 2 does not. Each of the populations has the same two processes shown in Scheme 1, but they may have different first order reactions; therefore, there are four rate constants possible as shown in Scheme 2. The data were

Scheme 2. Kinetic Model for the Global-Fitting Analysis of the Stopped-Flow Data in the Presence of 4-BP



globally fit to a fourth-exponential function according to the proposed kinetic model in Scheme 2, from which the rate constant k_I , k_{RH} , k_{i1} , k_{iRH} and the 3×5 C coefficient matrix was determined. The basis spectra, b-spectra (Figure S3), were calculated through $B = \text{USC}$ and the spectra corresponding to each intermediate were reconstructed based on the analytical solution of each kinetic model. The SVD and global fitting analysis were performed using Igor Pro 6.04 (Supporting Information).

The initial rates of a series of substrate and inhibitor concentrations were measured as a function of temperature. The slopes of experimental progress curves were determined using the method of initial rates by linear fit of the first ten time points to provide V_0 . The initial rates V_0 in the presence of inhibitor 4-BP were then analyzed according to eq 1, which was

derived from proposed 4-BP inhibited ping-pong mechanism based on the steady state assumption. Equation 1 was then simultaneously fit to all measured initial rates at different substrate and inhibitor concentrations using nonlinear regression. V_{max} was fit globally according to the proposed inhibition mechanism. K_m^{app} was then determined at each inhibitor concentration. Then a linear fit of K_m^{app} against inhibitor concentration $[4\text{-BP}]$ was conducted to determine the K_i . All the data analysis and fitting was conducted using Igor Pro 6.04.

RESULTS

The measurements were originally designed to address the effect of the inhibitor 4-BP on the turnover frequency using the Michaelis–Menten kinetic scheme. However, the data revealed a more complicated partial inhibition when the inhibitor is present at less than 10 equiv of DHP. This regime was investigated using stopped-flow kinetics in the absence of substrate (but with cosubstrate H_2O_2) in order to understand alternative pathways leading to inactivation of the enzyme. Finally, the temperature dependence of the kinetics at higher 4-BP concentrations was obtained using van't Hoff analysis to determine the thermodynamic parameters of the association of 4-BP with DHP.

Stopped-Flow Kinetics of the Reaction between Ferric DHP and H_2O_2 in the Presence of 4-BP. The reactions of DHP with H_2O_2 in the presence or absence of 4-BP were monitored by using a single-mixing stopped-flow UV–visible spectrophotometer. It has been shown that ferric DHP reacts with H_2O_2 forming Compound ES, an iron(IV)-oxo species with an amino acid radical located on one or more of the three tyrosines, Y28, Y34, and Y38,²⁹ in a pH-dependent mechanism.²⁸ The iron(IV)-oxo porphyrin π -cation radical species Compound I has not been observed in wild-type DHP for this reaction, although it has been observed in the Y28F,Y34F,Y38F triple mutant of DHP (data unpublished). In the absence of inhibitor 4-BP, ferric DHP reacted with 10 equiv of H_2O_2 at pH 7.0 yielding Compound ES. Compound ES formation reaches a maximum 2 s after mixing, and subsequently an inactivated DHP species, known as Compound RH, was formed on a time scale of 80 s (Figure 1a). The well-defined features of Compound ES have been characterized based on the spectra extracted from the SVD analysis (see Methods) in comparison to previous work.²⁷ The Soret band of compound ES is observed at 420 nm and a distinctive double-peaked Q-band is also evident with α and β bands at 546 and 586 nm, respectively. Compound RH has a Soret band at 411 nm and has a broad and featureless Q-band in the visible region with a λ_{max} at 540 nm.

Upon preincubation of DHP with 1–10 equiv of 4-BP and initiation of the reaction with 10 equiv of H_2O_2 , two parallel pathways are observed, which are distinguished as the 4-BP bound form and the unbound form. The origin of the two parallel pathways is simply that DHP is in equilibrium with 4-BP and there are two populations at the instant that the reaction is initiated by H_2O_2 . As expected, we observe that the 4-BP unbound form has the same kinetic parameters observed previously for the reaction of DHP with H_2O_2 . Both Compound ES and Compound RH have been observed in the reconstructed spectrum (Figure 1-b1,c1,d1) with similar rate constants, k_I and k_{RH} obtained from the fitting (Table 1). On the other hand, in the 4-BP bound form, a new species was observed that also possessed a double-peaked Q-band at 541

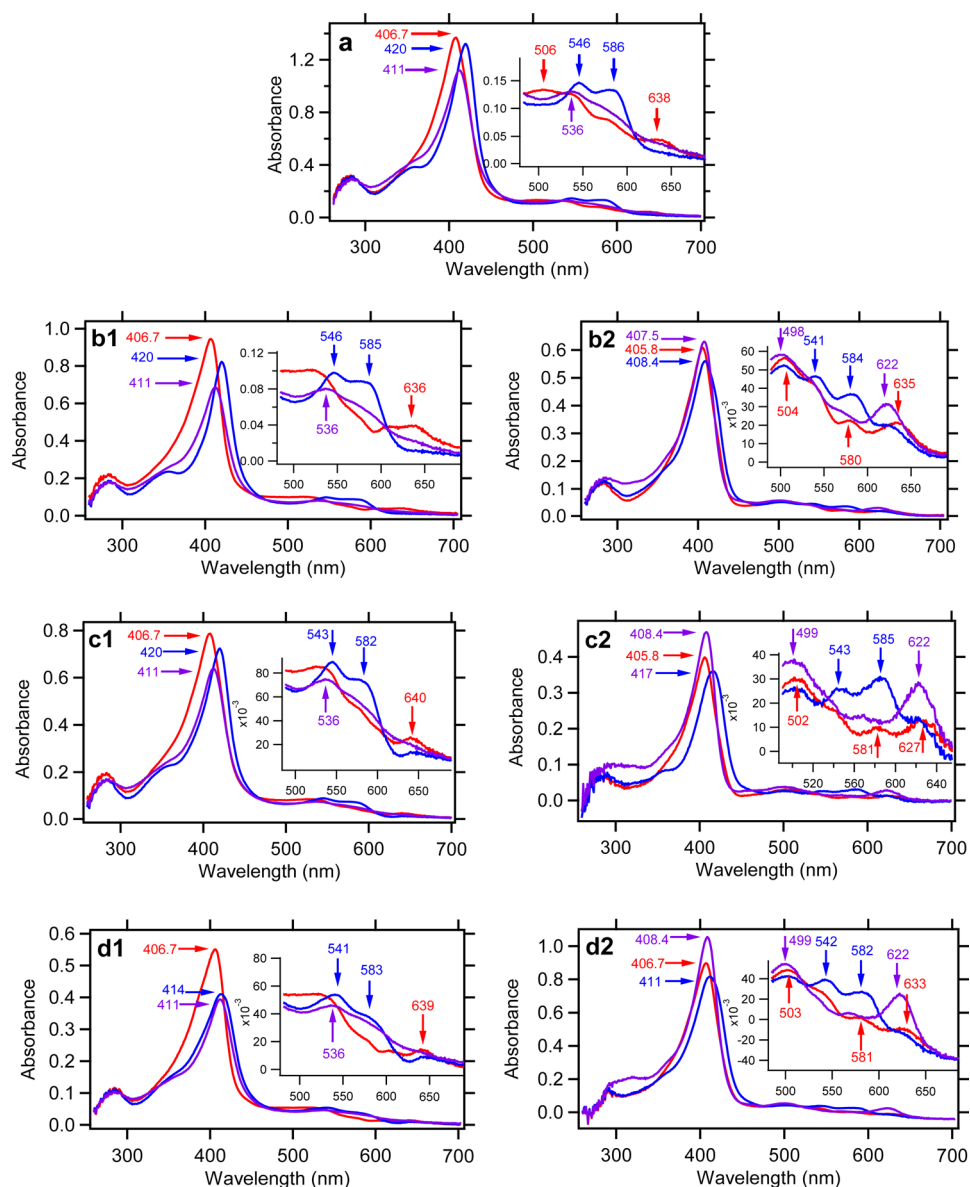


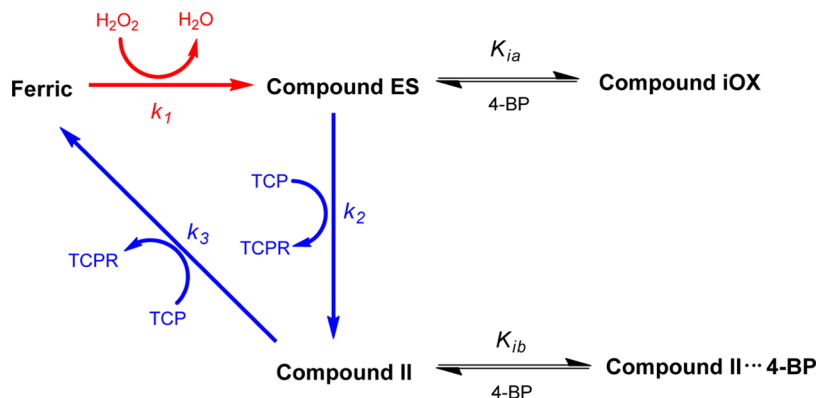
Figure 1. Calculated spectra from SVD analysis of the time-resolved UV–visible spectra. The measurements were conducted at $[DHP] = 10 \mu M$, $[H_2O_2] = 100 \mu M$ in the 100 mM K_P buffer pH 7.0 with (a) $0 \mu M$ 4-BP; (b) $10 \mu M$ 4-BP; (c) $20 \mu M$ 4-BP; (d) $100 \mu M$ 4-BP. In the presence of 4-BP, two parallel kinetic pathways are observed, which are distinguished by the 4-BP bound and unbound forms of DHP. Thus, (b1), (c1), and (d1) represents the 4-BP unbound pathway; (b2), (c2), and (d2) represent the 4-BP bound pathway. The red, blue, and purple curves in (a), (b1), (c1), and (d1) represent ferric DHP, Compound ES, and Compound RH, respectively. Along the pathway for inhibitor-bound DHP, the red, blue, and purple curves in panels (b2), (c2), and (d2), represent ferric DHP, Compound iOX, and Compound iRH, respectively.

Table 1. Kinetic Parameters Obtained from Global-Fitting of Evolutionary Time-Course

[4-BP] (μM)	k_1 (s^{-1})	k_{RH} (s^{-1})	k_{iI} (s^{-1})	k_{iRH} (s^{-1})
0	2.78 ± 0.78	0.031 ± 0.001		
10	2.59 ± 0.10	0.017 ± 0.005	5.67 ± 2.43	0.276 ± 0.072
20	3.09 ± 0.19	0.041 ± 0.001	6.29 ± 0.44	0.393 ± 0.009
100	2.88 ± 1.51	0.073 ± 0.020	6.35 ± 0.90	0.536 ± 0.040

and 584 nm (1 equiv 4-BP), 543 and 585 nm (2 equiv 4-BP), and 541 and 583 nm (10 equiv 4-BP), while the Soret band at 408.4 nm (1 equiv 4-BP), 417 nm (2 equiv 4-BP), and 411 nm (10 equiv 4-BP). The different Soret bands obtained from calculated spectra may imply the existence of equilibrium between Compound ES and Compound iOX in the presence of

4-BP, which introduces uncertainty in the determination of the linear combinations of b-spectra to reconstruct the intermediate spectra. Since the Soret bands in the 4-BP-bound species are not the same as those for uninhibited DHP, we refer to the intermediate in this 4-BP-bound form as Compound iOX. The nomenclature is based on the fact that the intermediate is in equilibrium with the intermediate compound ES when inhibitor bound in the distal pocket, but does not necessarily mean both intermediates share the oxo-ferryl heme structure. The spectrum of the end-point for the assay also shows that another new species with a Soret band at 407.5 nm and distinct charge-transfer band at 622 nm has formed. This form has been named Compound iRH (Figure 1-b2,c2,d2). The names compound iOX and iRH imply that the most significant difference with respect to compound ES and RH is the

Scheme 3. Ping Pong Scheme for the Reaction of DHP with Substrate TCP^a

^aThe rate scheme incorporates nonclassical competitive inhibition in presence of inhibitor 4-BP.

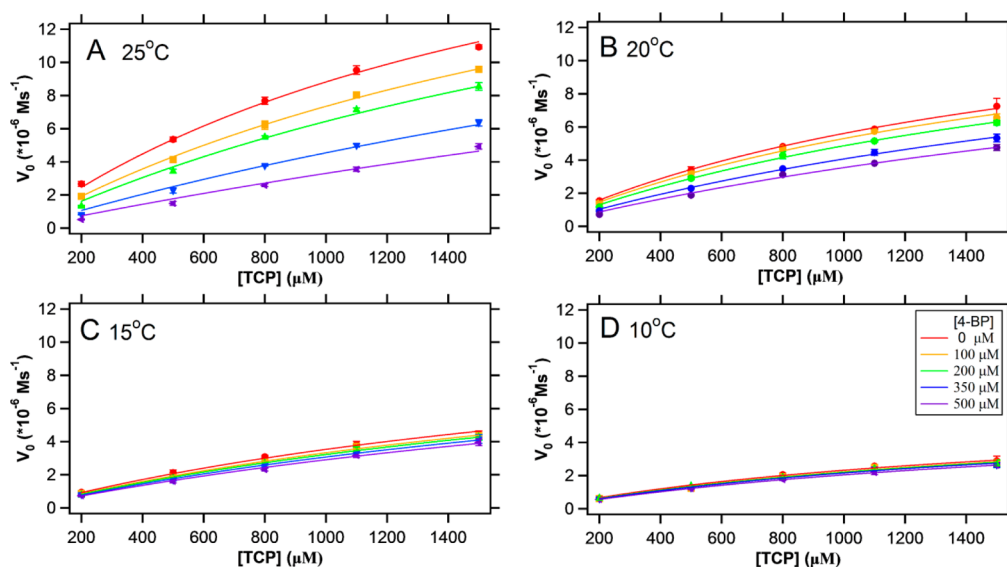


Figure 2. Bench-top mixing kinetic analysis of DHP catalyzed TCP oxidation reaction inhibited by 4-BP at different temperatures (a) 25 °C, (b) 20 °C, (c) 15 °C, and (d) 10 °C. Kinetic assay conditions were ferric DHP = 2.4 μM, H₂O₂ = 1200 μM in 100 mM KP_i buffer, pH 7.0.

presence of the inhibitor in the distal pocket. Since little or no ferryl intermediate is formed when 4-BP is bound in the distal pocket, we have used the designation iOX to signify that there is oxidation by H₂O₂, but it may involve a different mechanism. Both k_{iI} and k_{iRH} that correspond to the formation of Compound iOX and Compound iRH slightly increase as the concentration of 4-BP increases. Compared with k_I and k_{RH} , k_{iI} is about 2-fold larger than k_I , and k_{iRH} is about 10-fold larger than k_{RH} .

Bench-Top Mixing Kinetics with Substrate 2,4,6-TCP and Inhibitor 4-BP. The kinetic model given in eqs 1–3 was derived from combination of previous DHP catalytic kinetic model¹⁸ and the inhibition mechanism proposed above (Scheme 2). The previous DHP catalytic kinetic model is an application of the steady-state approximation to both compound ES and compound II formation in the classic peroxidase rate scheme. The steady-state approximation was invoked to derive a simplified ping pong scheme with nonclassical competitive inhibition. In the inhibition model, we believe that the inhibition does not take place when 4-BP binds to ferric DHP, but rather at the step where Compound iOX/Compound II...4-BP form. K_{ia} and K_{ib} correspond to the 4-BP dissociation constants of Compound iOX and Compound

II...4-BP, respectively. Since Compound ES and Compound II are two subsequent active enzyme intermediates during the two consecutive one-electron steps, we cannot distinguish between the binding and inhibitory effects of 4-BP on these two intermediates in our steady-state inhibition kinetic analysis. Therefore, we propose that the binding interaction of 4-BP will exert the same inhibitory effects on both compounds ES and II, which leads to the assumption that $K_{ia} = K_{ib} = K_i$. Equation 1 was derived based on the steady state approximation applied to Compound iOX and Compound II...4-BP, which are the forms of compounds ES and II in the presence of inhibitor 4-BP.

$$V_0 = \frac{k_{cat}[E]_0[TCP]}{K_m \left(1 + \frac{[4-BP]}{K_i} \right) + [TCP]} \quad (1)$$

$$k_{cat} = k_1[H_2O_2] \quad (2)$$

$$K_m = k_1[H_2O_2] \left(\frac{1}{k_2} + \frac{1}{k_3} \right) \quad (3)$$

Figure 2 presents the Michaelis–Menten curves of initial velocity V_0 vs substrate concentration, [TCP], at 25, 20, 15, and

10 °C. The inhibition effects of 4-BP on the DHP catalyzed substrate oxidation reaction were observed at each temperature. V_0 decreases as the inhibitor concentration is increased. However, the pattern of the Michaelis–Menten curves tends to converge to the uninhibited Michaelis–Menten curve as the temperature is decreased, which indicates a decrease in the inhibitory effect due to the temperature dependence of the inhibition constants, K_i , which are reported in Table 2. The values in Table 2 show that K_i decreases significantly as temperature increases, which means that the inhibitor is more potent at higher temperature.

Table 2. Michaelis-Menten Parameters from Bench-Top Mixing Kinetic Assay

T (K)	k_{cat} (s ⁻¹)	k_{cat}/K_m (s ⁻¹ mM ⁻¹)	K_i (mM)
283	2.57 ± 0.15	1.54 ± 0.02	2.560 ± 0.036
288	5.07 ± 0.25	2.04 ± 0.02	1.735 ± 0.016
293	6.40 ± 0.28	3.95 ± 0.19	0.490 ± 0.024
298	10.42 ± 0.70	7.12 ± 1.57	0.155 ± 0.034

van't Hoff Analysis of the Inhibition Constant K_i . By measuring K_i at a series of temperatures, $\ln(K_i)$ vs $1/T$ in a van't Hoff plot was used to calculate ΔH^\ominus and ΔS^\ominus . Figure 3

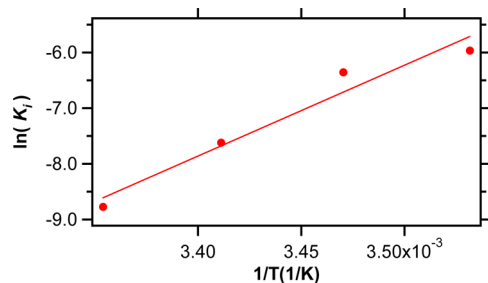


Figure 3. van't Hoff plot of $\ln(K_i)$ vs $1/T$ for inhibitor 4-BP binding to ferric DHP. The K_i value was determined at pH = 7 in 100 mM KP_i buffer. 2,4,6-TCP was used as the substrate.

shows a plot of $\ln(K_i)$ vs $1/T$ based on the van't Hoff equation, $-\ln(K_i) = \Delta G^\ominus/RT = \Delta H^\ominus/RT - \Delta S^\ominus/R$. Thus, $\Delta H^\ominus = -135.5 \pm 20.9$ kJ/mol and $\Delta S^\ominus = -526.1 \pm 71.9$ J/(mol·K) that corresponding to the enzyme–inhibitor complex dissociation process. The benchtop mixing kinetics shows that binding of 4-BP to DHP has an unfavorable positive enthalpy and a favorable positive entropy, which informs us that the binding process is entropy-driven. The free energy at temperatures of physiological interest are $\Delta G^\ominus = -21.28$ kJ/mol at $T = 298$ K.

DISCUSSION

DHP is a hemoglobin that exhibits levels of peroxidase activity comparable to typical peroxidases.¹⁷ DHP has been shown to be able to oxidize a variety of substituted phenols, such as the trihalophenols, dihalophenols, 4-chlorophenol, 4-fluorophenol, and a number of other substrates. However, the inhibition of DHP by 4-BP provokes an intriguing mechanistic question. How does DHP function in ecosystems where 4-BP is prevalent? The inhibitor 4-BP is a brominated secondary metabolite secreted by marine polychaetes that coexist with *A. ornata* in greater concentration than the substrate 2,4,6-TBP.¹³ The previously proposed inhibition mechanism placed emphasis on the internal distal pocket as the inhibitor binding site and the subsequent impact on the conformation of distal

His⁵⁵.¹² The distal His⁵⁵ has been shown to be essential for catalysis.^{32,33} Moreover, His⁵⁵ has also been shown to be unusually flexible in DHP, when compared to other globins, meaning that it exists nearly equally in two conformers at pH 6.³⁴ The existence of internal (closed) and external (open) conformers in globins such as Sperm Whale myoglobin has been shown to favor the internal conformation unless the pH is lowered to pH < 4.5.³⁵ One possible cause for inhibition in DHP is that 4-BP binding forces His⁵⁵ into the open conformation that is distant from the heme iron center, and thus no longer being able to function as an acid–base catalyst to facilitate heterolytic O–O bond cleavage. Therefore, significantly lower turnover of 4-BP bound ferric DHP to the active oxo-ferryl species would be expected in the presence of 4-BP based upon this mechanism. However, the data presented in this study reveal that not only is compound ES formed in the presence of 4-BP in the low concentration regime (<10 equiv) in the 4-BP unbound form of DHP. In fact, a new species Compound iOX with the rate constant k_{i1} that is about 2-fold of k_i is formed when 4-BP binds in the distal pocket. Despite the fact that the Compound ES formation rate constant, k_i , is not perturbed, the amount of compound ES decreases when inhibitor 4-BP is present, because of the formation of Compound iOX in an alternative pathway. Subsequently, Compound iOX is converted to the second new species Compound iRH with the rate constant, k_{iRH} that is 10-fold larger than k_{RH} . Thus, based upon the observed transient-state kinetics, we believe that the presence of 4-BP in the range from 1 to 10 equiv relative to DHP does not impede H₂O₂ entering the distal pocket. Rather, the effect of 4-BP appears to be a reduction of the rate of subsequent reactions, which may be binding of H₂O₂ to the heme Fe or the activation of bound H₂O₂. Thus, the inhibition of the catalytic turnover is due to the decreasing yield of Compound ES due to the existence of an alternative pathway in the 4-BP bound form.

Unlike Compound ES, Compound iOX does not clearly involve a ferryl species. Irrespective of the mechanism for activation of H₂O₂, there is clearly a change in heme structure following addition of H₂O₂, which suggests an alternative mechanism for oxidation in the 4-BP bound form. The iOX spectrum shown in Figure 1-b2 appears to have a small ferryl component, which means that a role for the heme Fe cannot be excluded. A second difference between ES and iOX is that 4-BP itself may participate in electron transfer reactions via a radical mechanism. While compound ES has been shown to be consistent of an ferryl heme with a tyrosine radical, we propose that compound iOX may involve a transient radical located on 4-BP (Figure 4). This hypothesis is plausible because the distance from the phenolic oxygen of 4-BP to heme iron is only 6.48 Å (Figure 5), which is less than the distance to either Tyr³⁴ (11.36 Å, Tyr phenolic oxygen) or Tyr³⁸ (9.48 Å, phenolic oxygen). Thus, if heme Fe is involved in any way in this process, which we deem likely, 4-BP should be more readily oxidized than any of tyrosines due to its proximity. In terms of the driving force—the free energy, the bond dissociation free energy (BDFE) of phenolic hydroxyl group of 4-BP is 6.7 kJ/mol higher than that of the tyrosine.³⁶ In other words, in terms of free energy, 4-BP is more stable than tyrosine. Thus, these two factors may counteract each other, which gives rise to similar rate constants for formation of Compound ES and Compound iOX.

A new species with a Soret band at 408 nm, Q-band maximum at 498 nm, and charge transfer band at 622 nm was

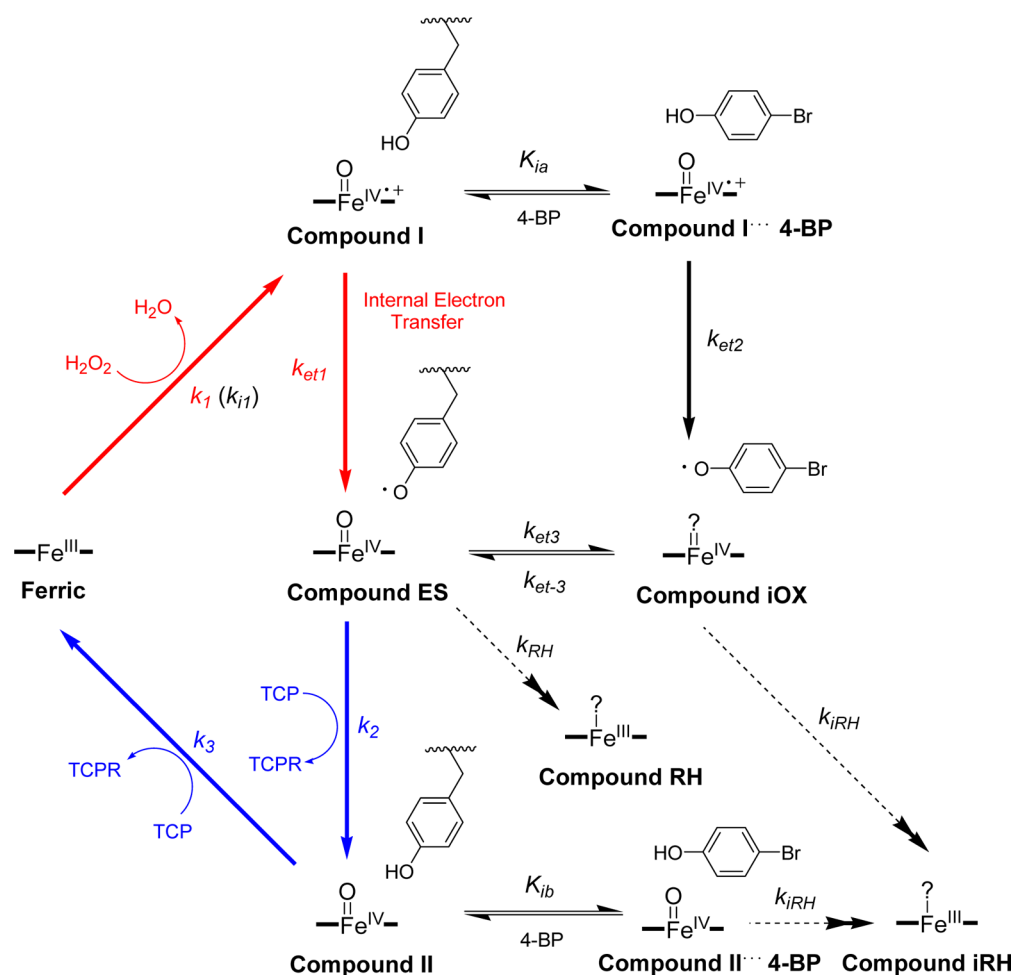


Figure 4. Proposed DHP catalytic cycle and inhibition mechanism in the presence of inhibitor 4-BP. The form of the heme Fe in compound iOX and iRH is not known and therefore marked with a question mark. Nonetheless, since the heme Soret band is altered in these species there is strong reason to believe that there have been changes that involve the Fe.

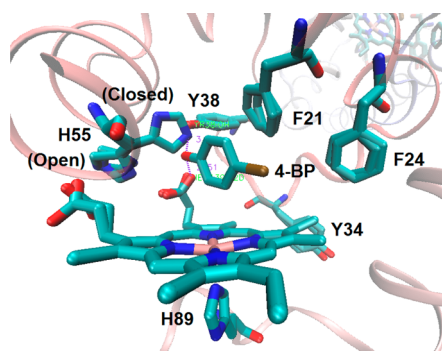


Figure 5. Structure of DHP in the presence of 4-BP as determined by X-ray crystallography (PDB 3LB2). The multiple positions of amino acids and propionate side chains in the structure are indicated in the figure.

formed in the presence of 4-BP. We assign this to the five-coordinated Compound iRH. Compound iRH is a unique species that is not equilibrated with Compound RH in the presence of 4-BP. Adding 4-BP to Compound RH does not give rise to Compound iRH (Figure S7). It is known that, for ferric DHP, internal binding of 4-BP lowers the population of the six-coordinated high spin heme and increases the population of five-coordinated high spin heme.²⁸ Moreover,

the charge-transfer band at 622 nm also indicates that 4-BP plays a role in forming a five-coordinate Compound iRH. In analogous fashion, it has been shown that the competitive inhibitor of horseradish peroxidase (HRP), benzohydroxamic acid (BHA), also affects the charge transfer band of the ferric HRP.³⁷ In the presence of BHA, the charge transfer band becomes stronger. In a manner analogous to BHA binding to HRP, the charge-transfer band at 622 nm becomes sharper and stronger as the concentration of 4-BP increases. It should be noted that, as an aromatic ligand, BHA binds at the β edge of the distal pocket above the heme.³⁸ However, the binding location of BHA in HRP is not nearly as deeply buried in the protein as 4-BP in DHP. The spectral differences between compound iRH and RH suggest that possibilities of cross-linked heme²⁷ and six-coordinate bis-histidine hemichrome still exist, but the Soret band is shifted due to the presence of an internally bound inhibitor.

Bench-top mixing kinetics have shown that the inhibition constant K_i has a strong temperature dependence. The value of K_i decreases by a factor of 3 for each increase in 5 °C. The large positive enthalpy and entropy calculated from the van't Hoff equation suggests that the binding of 4-BP is enthalpically unfavored and entropy-driven. The crystal structure of DHP with binding of inhibitor 4-XP (X = F, Cl, Br, I) shows that 4-XP is surrounded by the hydrophobic amino acid residues V59,

L100, F21, F24, and F35.¹⁴ Since 4-BP has $pK_a = 9.29$, it remains protonated at pH 7.0. Thus, the hydrophobic effect will give rise to a favorable entropy of binding in the distal pocket. In support of the dominance of the hydrophobic effect in the entropy, we note that 4-BP is not a highly flexible molecule. Thus, there is little conformational entropy change upon binding. Although the hydrogen bond interaction of 4-BP with Y38 and heme propionate D and π -stacking interaction between aromatic ring of 4-BP and F21 may contribute to the enthalpy, the binding also involves the displacement of a water molecule bound to the heme Fe atom and displacement of His⁵⁵ into solvent water, which are both enthalpically disfavored, but entropically favored.³⁹ The desolvation of 4-BP as it binds in an internal hydrophobic pocket is most likely the major contribution to the positive entropy change of binding.

The inhibition constant K_i is a dissociation constant of the enzyme–inhibitor complex, thus we compare the K_d value with previously reported dissociation constant for 4-halophenol to DHP which was measured by Raman spectroscopy in the absence of H₂O₂ at pH 6.0. The dissociation constant follows the trend of size of the para halogen in 4-XP where X = I > Br > Cl > F > H, with the values of 0.536 mM, 1.15 mM, 1.78 mM, 3.72 mM, and 10 mM, respectively.¹² The K_d of 4-BP measured using the measurement by resonance Raman spectroscopy is 1.15 mM, which is within the range we measured from 283 to 298 K. However, it also must be understood that the K_d value measured by Raman reflects the interplay between 6cHS and 5cHS by disturbing the water ligation, and thus is only indirectly related to the binding of 4-BP.

The biological role of inhibition may be explained by consideration of the relative concentrations of 4-BP, 2,4-dibromophenol, and 2,4,6-TBP, which are typical secondary metabolites secreted by marine polychaetes. For example, *Notomastus lobatus*, excretes 4-BP, 2,4-dibromophenol, and 2,4,6-TBP to the surrounding environment with a stoichiometric ratio of 1.8:0.9:1.0.¹³ The reason DHP selectively oxidizes 2,4,6-TBP, but not 4-BP, may be partially the relative toxicity of these two compounds and their oxidized intermediates. 2,4,6-TBP has been shown to disrupt the function of cellular Ca²⁺ ion channel in neuroendocrine cell and may potentially disturb the endocrine system in invertebrates.⁴⁰ It also has a negative impact on the ability of polychaetes to burrow and feed.⁴¹ On the other hand, there is no known inhibitor effect of 4-BP on respiration and the assimilation of acetate or glucose by sediment bacteria, indicating that it has significantly lower toxicity relative to 2,4,6-TBP.⁴² Thus, we assume that the high priority for DHP to degrade 2,4,6-TBP is due to its high toxicity. Not only is 4-BP less toxic than 2,4,6-TBP, but oxidation of 4-BP can lead to polymerization of the radical intermediate, which may increase the toxicity relative to the starting phenol. This is distinct from the fate of 2,4,6-TXP radicals, which form quinones by disproportionation⁴³ and hydroxyquinones by a further radical pathway.⁴⁴ Thus, the differences in binding site and reactivity of 4-BP and 2,4,6-TBP may be an evolutionary consequence of the regulation of catalytic reactivity *in vivo*.

■ ASSOCIATED CONTENT

● Supporting Information

Singular value decomposition analysis and figures are presented. This material is available free of charge via the Internet at <http://pubs.acs.org>.

■ AUTHOR INFORMATION

Corresponding Author

*E-mail: Stefan_Franzen@ncsu.edu.

Notes

The authors declare no competing financial interest.

■ ACKNOWLEDGMENTS

This work was supporting by ARO grant LS-58761. We thank Dr. Reza Ghiladi for use of the stopped-flow UV–visible spectrophotometer to obtain the time-resolved spectra. Jing Zhao thanks Chenyue Hu for providing Python script for processing the stopped-flow time-resolved spectra data.

■ REFERENCES

- (1) Chen, Y. P.; Woodin, S. A.; Lincoln, D. E.; Lovell, C. R. An Unusual Dehalogenating Peroxidase from the Marine Terebellid Polychaete *Amphitrite ornata*. *J. Biol. Chem.* **1996**, *271*, 4609–12.
- (2) D'Antonio, J.; D'Antonio, E. L.; Thompson, M. K.; Bowden, E. F.; Franzen, S.; Smirnova, T.; Ghiladi, R. A. Spectroscopic and Mechanistic Investigations of Dehaloperoxidase B from *Amphitrite ornata*. *Biochemistry* **2010**, *49*, 6600–6616.
- (3) Zamocky, M.; Gasselhuber, B.; Furtmuller, P. G.; Obinger, C. Molecular Evolution of Hydrogen Peroxide Degrading Enzymes. *Arch. Biochem. Biophys.* **2012**, *525*, 131–144.
- (4) Weber, R. E.; Mangum, C.; Steinman, H.; Bonaventura, C.; Sullivan, B.; Bonaventura, J. Hemoglobins of Two Terebellid Polychaetes: *Enoplobranchus sanguineus* and *Amphitrite ornata*. *Comp. Biochem. Physiol. A: Comp. Physiol.* **1977**, *56*, 179–87.
- (5) Menale, C.; Nicolucci, C.; Catapane, M.; Rossi, S.; Bencivenga, U.; Mita, D. G.; Diano, N. Optimization of Operational Conditions for Biodegradation of Chlorophenols by Laccase-polyacrylonitrile Beads System. *J. Mol. Catal. B-Enzym.* **2012**, *78*, 38–44.
- (6) Franzen, S.; Gilvey, L. B.; Belyea, J. L. The pH Dependence of the Activity of Dehaloperoxidase from *Amphitrite ornata*. *Biochim. Biophys. Acta-Prot. Proteom.* **2007**, *1774*, 121–130.
- (7) Davis, M. F.; Gracz, H.; Vendeix, F. A. P.; de Serrano, V.; Somasundaram, A.; Decatur, S. M.; Franzen, S. Different Modes of Binding of Mono-, Di-, and Trihalogenated Phenols to the Hemoglobin Dehaloperoxidase from *Amphitrite ornata*. *Biochemistry* **2009**, *48*, 2164–2172.
- (8) Raven, E. Peroxidase-Catalyzed Oxidation of Ascorbate Structural, Spectroscopic and Mechanistic Correlations in Ascorbate Peroxidase Enzyme-Catalyzed Electron and Radical Transfer; Holzenburg, A., Scrutton, N., Eds.; Springer, 2002; Vol. 35, pp 317–349.
- (9) Zamocky, M.; Furtmuller, P. G.; Obinger, C. Evolution of Structure and Function of Class I Peroxidases. *Arch. Biochem. Biophys.* **2010**, *500*, 45–57.
- (10) Bailly, X.; Chabasse, C.; Hourdez, S.; Dewilde, S.; Martial, S.; Moens, L.; Zal, F. Globin Gene Family Evolution and Functional Diversification in Annelids. *FEBS J.* **2007**, *274*, 2641–2652.
- (11) Osborne, R. L.; Coggins, M. K.; Raner, G. M.; Walla, M.; Dawson, J. H. The Mechanism of Oxidative Halophenol Dehalogenation by *Amphitrite ornata* Dehaloperoxidase Is Initiated by H₂O₂ Binding and Involves Two Consecutive One-Electron Steps: Role of Ferryl Intermediates. *Biochemistry* **2009**, *48*, 4231–4238.
- (12) Thompson, M. K.; Davis, M. F.; de Serrano, V.; Nicoletti, F. P.; Howes, B. D.; Smulevich, G.; Franzen, S. Internal Binding of Halogenated Phenols in Dehaloperoxidase-Hemoglobin Inhibits Peroxidase Function. *Biophys. J.* **2010**, *99*, 1586–1595.
- (13) Lincoln, D. E.; Fielman, K. T.; Marinelli, R. L.; Woodin, S. A. Bromophenol Accumulation and Sediment Contamination by the Marine Annelids *Notomastus lobatus* and *Thelepus crispus*. *Biochem. System. Ecol.* **2005**, *33*, 559–570.
- (14) de Serrano, V.; Franzen, S. Structural Evidence for Stabilization of Inhibitor Binding by a Protein Cavity in the Dehaloperoxidase-hemoglobin from *Amphitrite ornata*. *Pept. Sci.* **2012**, *98*, 27–35.

- (15) Davydov, R.; Osborne, R. L.; Shanmugam, M.; Du, J.; Dawson, J. H.; Hoffman, B. M. Probing the Oxyferrous and Catalytically Active Ferryl States of *Amphitrite ornata* Dehaloperoxidase by Cryoreduction and EPR/ENDOR Spectroscopy. Detection of Compound I. *J. Am. Chem. Soc.* **2010**, *132*, 14995–15004.
- (16) Osborne, R. L.; Coggins, M. K.; Walla, M.; Dawson, J. H. Horse Heart Myoglobin Catalyzes the H₂O₂-Dependent Oxidative Dehalogenation of Chlorophenols to DNA-Binding Radicals and Quinones. *Biochemistry* **2007**, *46*, 9823–9829.
- (17) Belyea, J.; Gilvey, L. B.; Davis, M. F.; Godek, M.; Sit, T. L.; Lommel, S. A.; Franzen, S. Enzyme Function of the Globin Dehaloperoxidase from *Amphitrite ornata* Is Activated by Substrate Binding. *Biochemistry* **2005**, *44*, 15637–15644.
- (18) Ma, H.; Thompson, M. K.; Gaff, J.; Franzen, S. Kinetic Analysis of a Naturally Occurring Bioremediation Enzyme: Dehaloperoxidase-hemoglobin from *Amphitrite ornata*. *J. Phys. Chem. B* **2010**, *114*, 13823–9.
- (19) Sharp, K. H.; Moody, P. C. E.; Brown, K. A.; Raven, E. L. Crystal Structure of the Ascorbate Peroxidase-Salicylhydroxamic Acid Complex. *Biochemistry* **2004**, *43*, 8644–8651.
- (20) Davis, M. F.; Bobay, B. G.; Franzen, S. Determination of Separate Inhibitor and Substrate Binding Sites in the Dehaloperoxidase-Hemoglobin from *Amphitrite ornata*. *Biochemistry* **2010**, *49*, 1199–1206.
- (21) Zhao, J.; de Serrano, V.; Zhao, J.; Le, P.; Franzen, S. Structural and Kinetic Study of an Internal Substrate Binding Site in Dehaloperoxidase-Hemoglobin A from *Amphitrite ornata*. *Biochemistry* **2013**, *52*, 2427–2439.
- (22) D'Antonio, J.; Ghiladi, R. A. Reactivity of Deoxy- and Oxyferrous Dehaloperoxidase B from *Amphitrite ornata*: Identification of Compound II and Its Ferrous-Hydroperoxide Precursor. *Biochemistry* **2011**, *50*, 5999–6011.
- (23) Denisov, I. G.; Makris, T. M.; Sligar, S. G. Formation and Decay of Hydroperoxo-Ferric Heme Complex in Horseradish Peroxidase studied by Cryoradiolysis. *J. Biol. Chem.* **2002**, *277*, 42706–42710.
- (24) Miller, V. P.; Goodin, D. B.; Friedman, A. E.; Hartmann, C.; Demontellano, P. R. O. Horseradish Peroxidase Phe(172)-Tyr Mutant - Sequential Formation of Compound-I with a Porphyrin Cation and a Protein Radical. *J. Biol. Chem.* **1995**, *270*, 18413–18419.
- (25) Aisen, P. Identification by ENDOR of Trp191 as the Free-Radical Site in Cytochrome c Peroxidase Compound ES. *Chemtracts: Biochem. Mol. Biol.* **1990**, *1*, 441–3.
- (26) Goodin, D. B.; Mauk, A. G.; Smith, M. Studies of the Radical Species in Compound ES of Cytochrome c Peroxidase Altered by Site-Directed Mutagenesis. *Proc. Natl. Acad. Sci. U. S. A.* **1986**, *83*, 1295–1299.
- (27) Feducia, J.; Dumariéh, R.; Gilvey, L. B. G.; Smirnova, T.; Franzen, S.; Ghiladi, R. A. Characterization of Dehaloperoxidase Compound ES and Its Reactivity with Trihalophenols. *Biochemistry* **2009**, *48*, 995–1005.
- (28) Thompson, M. K.; Franzen, S.; Ghiladi, R. A.; Reeder, B. J.; Svistunenko, D. A. Compound ES of Dehaloperoxidase Decays via Two Alternative Pathways Depending on the Conformation of the Distal Histidine. *J. Am. Chem. Soc.* **2010**, *132*, 17501–17510.
- (29) Franzen, S.; Thompson, M. K.; Ghiladi, R. A. The Dehaloperoxidase Paradox. *Biochim. Biophys. Acta* **2012**, *1824*, 578–588.
- (30) Georgiadis, K. E.; Jhon, N.-I.; Einarsdottir, O. Time-Resolved Optical Absorption Studies of Intramolecular Electron Transfer in Cytochrome c Oxidase. *Biochemistry* **1994**, *33*, 9245–9256.
- (31) Rittle, J.; Younker, J. M.; Green, M. T. Cytochrome P450: The Active Oxidant and Its Spectrum. *Inorg. Chem.* **2010**, *49*, 3610–3617.
- (32) Franzen, S.; Belyea, J.; Gilvey, L. B.; Davis, M. F.; Chaudhary, C. E.; Sit, T. L.; Lommel, S. A. Proximal Cavity, Distal Histidine, and Substrate Hydrogen-Bonding Mutations Modulate the Activity of *Amphitrite ornata* Dehaloperoxidase. *Biochemistry* **2006**, *45*, 9085–9094.
- (33) Zhao, J. J.; de Serrano, V.; Dumariéh, R.; Thompson, M.; Ghiladi, R. A.; Franzen, S. The Role of the Distal Histidine in H₂O₂ Activation and Heme Protection in both Peroxidase and Globin Functions. *J. Phys. Chem. B* **2012**, *116*, 12065–12077.
- (34) Chen, Z.; de Serrano, V.; Betts, L.; Franzen, S. Distal Histidine Conformational Flexibility in Dehaloperoxidase from *Amphitrite ornata*. *Acta Crystallogr., Sect. D: Biol. Crystal.* **2009**, *D65*, 34–40.
- (35) Yang, F.; Phillips, G. N., Jr. Crystal structures of CO-, deoxy- and Met-Myoglobins at Various pH Values. *J. Mol. Biol.* **1996**, *256*, 762–774.
- (36) Warren, J. J.; Tronic, T. A.; Mayer, J. M. Thermochemistry of Proton-Coupled Electron Transfer Reagents and its Implications. *Chem. Rev.* **2010**, *110*, 6961–7001.
- (37) Zelent, B.; Kaposi, A. D.; Nucci, N. V.; Sharp, K. A.; Dalosto, S. D.; Wright, W. W.; Vanderkooi, J. M. Water Channel of Horseradish Peroxidase Studied by the Charge-Transfer Absorption Band of Ferric Heme. *J. Phys. Chem. B* **2004**, *108*, 10317–10324.
- (38) Gumiero, A.; Murphy, E. J.; Metcalfe, C. L.; Moody, P. C. E.; Raven, E. L. An Analysis of Substrate Binding Interactions in the Heme Peroxidase Enzymes: A Structural Perspective. *Arch. Biochem. Biophys.* **2010**, *13*–20.
- (39) de Serrano, V.; Chen, Z. X.; Davis, M. F.; Franzen, S. X-ray Crystal Structural Analysis of the Binding Site in the Ferric and Oxyferrous Forms of the Recombinant Heme Dehaloperoxidase Cloned from *Amphitrite ornata*. *Acta Crystallogr., Sect. D: Biol. Crystal.* **2007**, *63*, 1094–1101.
- (40) Hassenklover, T.; Predehl, S.; Pilli, J.; Ledwolorz, J.; Assmann, M.; Bickmeyer, U. Bromophenols, Both present in Marine Organisms and in Industrial Flame Retardants, Disturb Cellular Ca²⁺ Signaling in Neuroendocrine Cells (PC12). *Aquat. Toxicol.* **2006**, *76*, 37–45.
- (41) Fielman, K. T.; Woodin, S. A.; Walla, M. D.; Lincoln, D. E. Widespread Occurrence of Natural Halogenated Organics among Temperate Marine Infauna. *Marine Ecol.-Prog. Ser.* **1999**, *181*, 1–12.
- (42) Lovell, C. R.; Steward, C. C.; Phillips, T. Activity of Marine Sediment Bacterial Communities Exposed to 4-bromophenol, a Polychaete Secondary Metabolite. *Marine Ecol.-Prog. Ser.* **1999**, *179*, 241–246.
- (43) Sturgeon, B. E.; Battenburg, B. J.; Lyon, B. J.; Franzen, S. Revisiting the Peroxidase Oxidation of 2,4,6-Trihalophenols: ESR Detection of Radical Intermediates. *Chem. Res. Toxicol.* **2011**, *24*, 1862–1868.
- (44) Franzen, S.; Sasan, K.; Sturgeon, B. E.; Lyon, B. J.; Battenburg, B. J.; Gracz, H.; Dumariah, R.; Ghiladi, R. Nonphotochemical Base-Catalyzed Hydroxylation of 2,6-Dichloroquinone by H₂O₂ Occurs by a Radical Mechanism. *J. Phys. Chem. B* **2011**, *116*, 1666–1676.